Locomotive Wheel Speed Measurement under Wheel Slip Conditions

O. Zoubek, P. Pichlik, J. Zděnek, and J. Lettl
Department of Electric Drives and Traction, Faculty of Electrical Engineering
Czech Technical University in Prague, Technická 2, 166 27 Prague 6, Czech Republic

Abstract— Wheel speed of heavy freight train locomotive under non-ideal traction conditions was measured with very high resolution and fine precision. Many authors published papers in this area over past century, but only recent advance in the information technology enabled measurement in such extent and resolution at the same time. Most modern locomotives have the speed sensor coupled with the traction motor. Unlike many other authors doing research in the area of wheel-slip, in the presented case the wheel speed was measured directly on the wheel, not indirectly on the traction motor. This approach made it possible to observe the wheel speed directly, without the requirement to implement motor — wheel model, which can introduce inaccuracies. Thanks to an independent method of train speed determination using a sensitive GPS receiver, wheel slip speeds were identified accurately regardless of synchronous slip phenomenon. Despite the adhesion theory, three types of operation mode were identified: the stable traction with negligible slip without oscillations, the semi-stable traction with evident slip and oscillations, and the prominent wheel slip. As the wheel speed was measured directly on the wheel, much larger oscillations than ever published were revealed. The source of the oscillations is discussed in the paper. A simple MatLab model of rotational masses was constructed and tuned to match the measurements. Eigenvalues and eigenvectors of the model are discussed, too. The model of rotational masses is completed with adhesion model to perform simulation. The simulation results are presented and compared with the results of measurement.

1. INTRODUCTION

Advances and development in technology produces pressure on better utilization of resources. The pressure is present also in the field of railway traction to utilize better the available adhesion of traction vehicles. Better utilization of available traction vehicle adhesion is desirable in all main areas of railway transportation as commuter trains, heavy freight trains, as well as high-speed trains. In this area have been published many articles focusing on detection of wheel slip and algorithms for slip protection or slip controller. Authors are faced with the problem how to implement such advanced slip controller into a heavy freight locomotive. For the purpose of current status identification a measurement on a twenty years old locomotive was performed. The collected data do not match simulations or previously by other authors published findings [1, 4, 5].

2. MEASUREMENT SETUP

The wheel speed measurement was set up on a heavy freight train locomotive Skoda 93E. The locomotive has axle arrangement Bo'Bo'Bo' with nominal axle load of 20 tons. The motivation for the measurement was to hunt down inaccuracies in the speed measurements. The last measurement setup was under moderate adhesion conditions during regular service.

As depicted in Fig. 1, the locomotive has six axles, each axle is driven by a DC motor through a gearbox. The wheel which is closer to the gearwheel is the direct-driven wheel (DDW), the wheel which is further from the gearwheel is the indirect-driven wheel (IDW). On each axle is a speed measurement cogwheel with induction proximity sensor. According to the figure, the speed sensor is either on the left side or on the right side of the locomotive. The position of the speed sensor cogwheel plays significant role in the measurement dependent on whether the speed sensor is closer to the direct-driven or indirect-driven wheel. Signal from each speed sensor was caught on the cable from each bogie on the interface connector near the locomotive computer using an interface card inserted between the cable and the computer. All six speed signals were then connected to a logic analyzer.

Many papers published in the last century relates to the measurement regarding rail-wheel adhesion, but only recent advances in information technology have enabled measurement in extent achieved by the authors. The logic analyzer was setup to measure signals of all speed sensors simultaneously with resolution of 5 ns and the analyzer was capable to run the measurement during

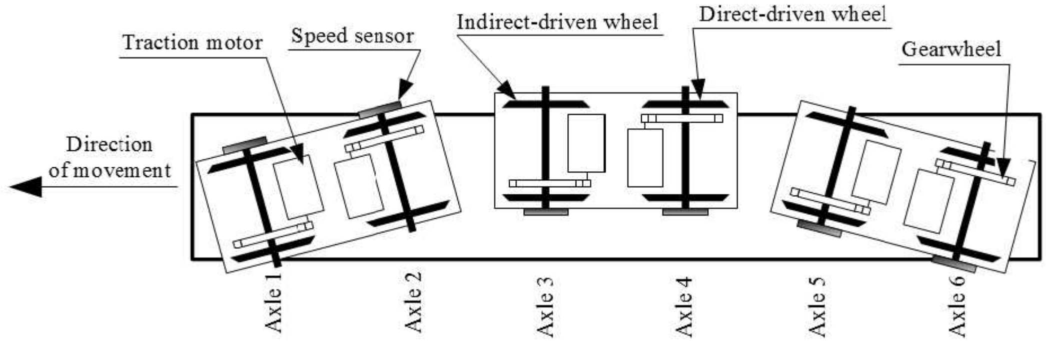

Figure 1: Arrangement of axles and speed sensor position.

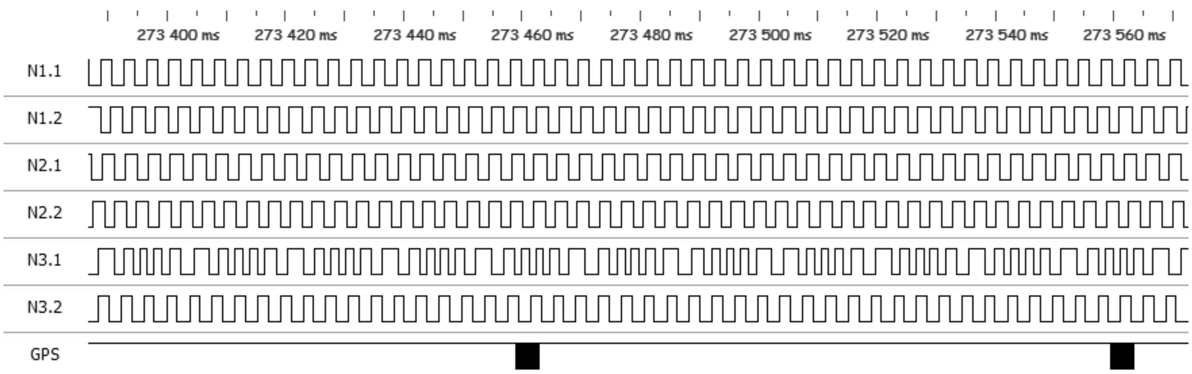

Figure 2: Sample of the data from the logic analyzer.

the whole test run. It allowed unprecedented resolution and length of the measurement. A sample data from the logic analyzer with prominent wheel slip are shown in Fig. 2.

A satellite navigation system with high accuracy and refresh rate receiving both GPS and GLONASS signal was installed on the roof of the locomotive. The receiver provided another independent method of determination of train speed with refresh rate of 10 Hz. Authors selected this method because the test run was performed in an open landscape with minimum number of obstacles such as tall buildings, underpasses and tunnels. Authors are aware that the method is inappropriate for train speed determination in deployment, but for the performed test run the method was sufficient.

3. SPEED SENSOR POSITION

On a modern locomotive with traction machine being AC induction motor (ACIM) is speed sensor coupled with the machine. This is a common requirement for a field-oriented control (FOC) of the ACIM. Because the speed sensor is already fitted on the machine, there is no demand to put it also on the wheel (either indirect-driven or direct-driven) because for static case a simple conversion over gearbox ratio gives correct wheel speed information.

Mechanical properties of the traction torque transmission system between the machine and the wheels considerably affect the usability of the speed sensor information as wheel speed information. Vibrations between the motor and wheels were researched [2] and also methods for reducing these vibrations were published [1]. The vibrations considered by previous authors were vibrations measured by the speed sensor coupled with the ACIM. Simulations indicate that the vibrations are between the machine and wheels.

As depicted in Fig. 3, authors performed the measurement on a locomotive with DC machine at typical arrangement of speed sensor used in case of this locomotive type, with the sensor coupled on a wheel. The measurement was done on each axle, therefore data for sensors both on the indirect-driven wheel and on the direct-driven wheel are available. The speed sensor is on either side of each axle, data for both sides of one axle are not currently available.

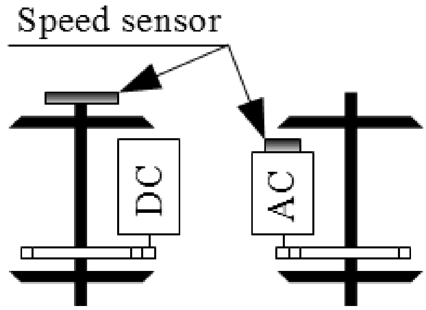

Figure 3: Typical speed sensor placement on AC and DC machines.

4. MACHINE — WHEEL VIBRATIONS

By means of simulations and simplified physical models many authors present phenomenon of vibrations between the machine and the wheels. They differ in frequency of the vibrations, but agree that the frequency depends on the machine size (mainly the difference between AC and DC motor) and on the method of machine mounting [1, 3, 4]. Such typical vibration simulation results are presented in Fig. 4 [4]. The simulation shows rising torque of the machine (T_w), vibrations of torque between the wheel and machine (T_k) torque on the wheel (T) as well as speed of the wheel (V_k) and speed of the train (V_p).

A very simplified three-masses model of the torque transmission is depicted in Fig. 5. This model can be used for majority of locomotives where the model is determined by alternating values only. At similar construction of the bogie parameters J_2, J_3, c_{23} and d_{23} remain similar for different types of locomotives. Larger variations can be found in parameters J_1, c_{12} and d_{12} that represent the motor moment of inertia and the gearbox properties. The used parameters are of BR120 published in [2, 3] and partly of Skoda 65E and 71E published in [4]. Authors of this paper do not have the exact parameters for Skoda 93E under test.

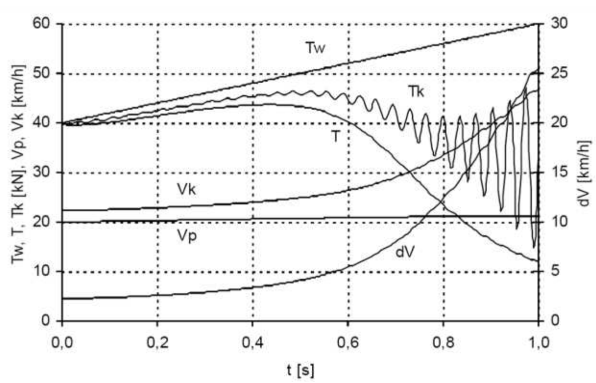

Figure 4: Vibrations according to Danzer.

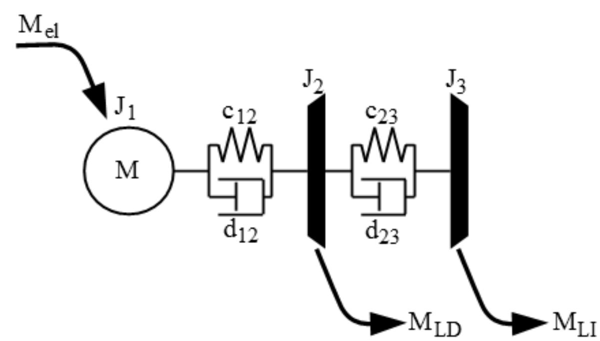

Figure 5: Three-masses model of torque transmission.

Vibrations on two different frequencies were identified in the data measured on Skoda 93E. The vibrations are prominent during slips. In Fig. 7 are depicted measured vibrations during a slip. Two waveforms are presented, one without a filter and the second one with a low-pass filter filtered out higher frequencies. Presence of two frequencies is consistent with the three-masses model of the torque transmission system expecting two pairs of complex conjugate eigenvalues. The known model of similar locomotives was tuned to obtain eigenvalues of 18 Hz and 61 Hz, the frequencies of Fig. 7.

Model parameters are following:

$c_{12} = 0.17 \times 10^6 \times p^2$ Nm/rad.
$d_{12} = 240 \times p^2$ Nms/rad.
$c_{23} = 11 \times 10^6$ Nm/rad.
$d_{23} = 74$ Nms/rad.

$J_1 = 40 \times p^2\,\mathrm{kgm}^2$.
$J_2 = 190\,\mathrm{kgm}^2$.
$J_3 = 130\,\mathrm{kgm}^2$.
$p = 81/18$ (gearbox ratio).

The eigenvectors of the resulting model are depicted in Fig. 6. This model eigenvalues clarify that the vibrations of 61 Hz are almost entirely distributed between J_2 and J_3 (i.e., the wheels) only. This could be one of the reasons why the other authors did not detect this type of vibrations before when measuring speed (and vibrations) directly on the machine. In steady state with constant speed and tractive effort, the torque M_{EL} given by the machine is in equilibrium with $M_{LD} + M_{LI}$. The torque distributed between M_{LD} and M_{LI} depends on adhesion conditions under each wheel (and speed of each wheel). Assuming $M_{LD} = M_{LI}$, the system is observable and angular speeds ω_2 and ω_3 can be estimated [2]. The measurement results show that this simplification is too significant and the vibrations between the wheels and the distribution of tractive force between the wheels may affect the adhesion by more than believed.

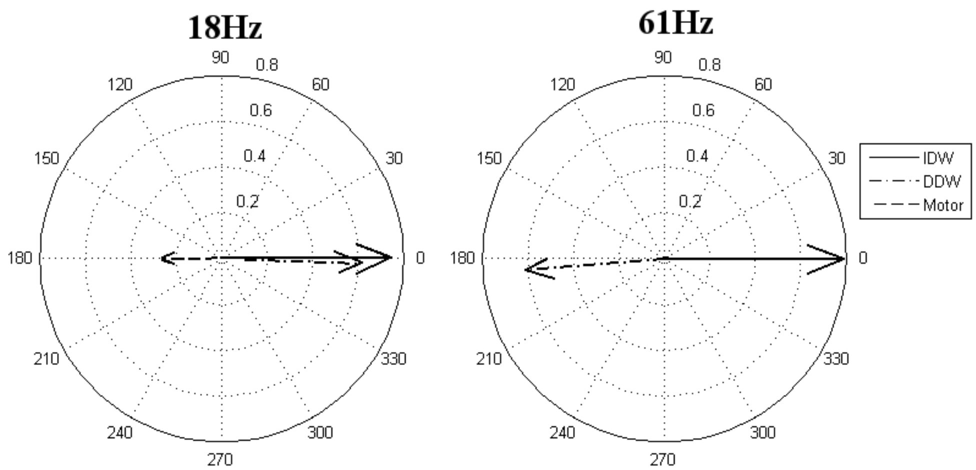

Figure 6: Eigenvectors of the three-masses model.

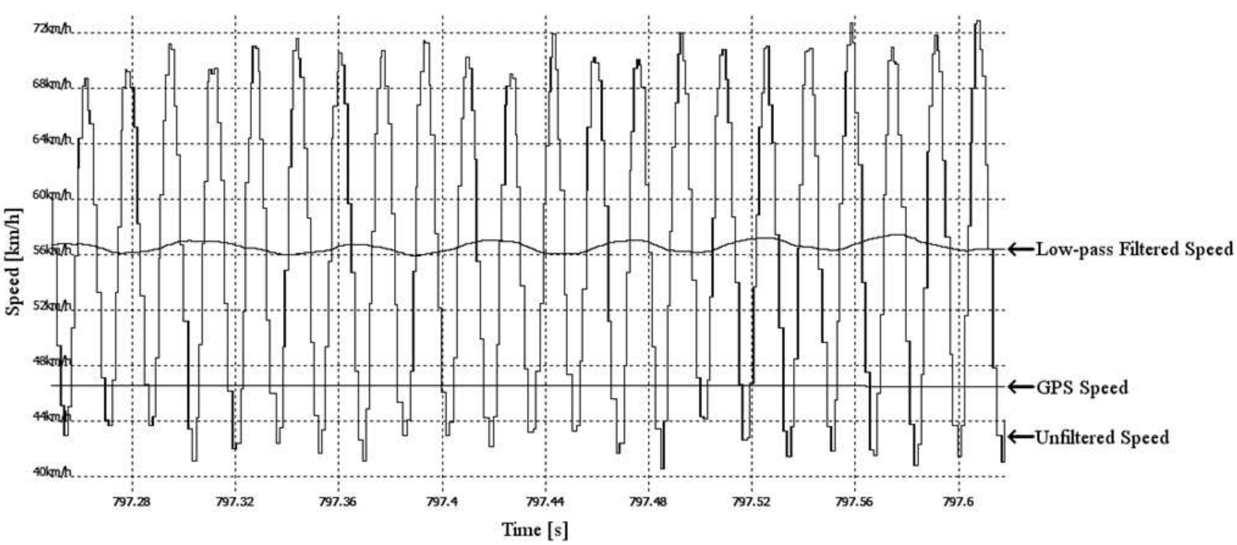

Figure 7: Vibrations in measured data at 61 Hz and 18 Hz.

5. MEASUREMENT

Speed measurement in a railway curve is always disturbed by non-ideal wheel guidance. Therefore the vibrations were studied only in the straight sections of the track.

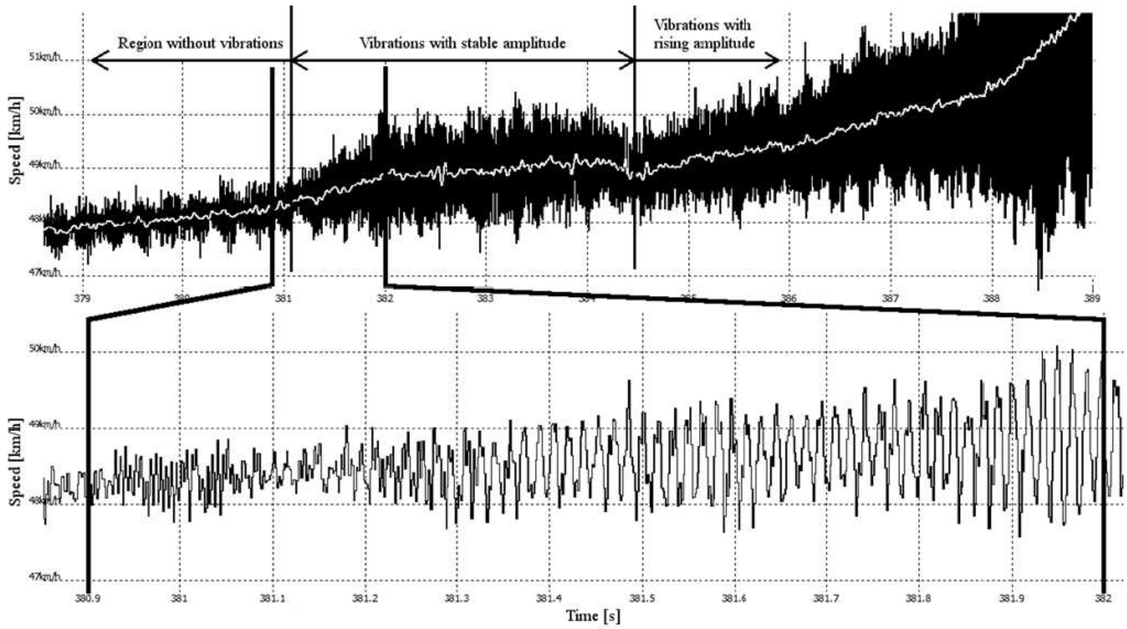

Figure 8: Three modes of operation on wheel-rail contact.

Three different modes of traction operation were identified during high tractive effort. All three modes of the operation are depicted within Fig. 8. The tractive force is constant during the whole period of time (i.e., the slip controller did not react until end of Fig. 8). The identified modes of operation are:

1. The first mode with no vibrations and very small slip speed ($s = \Delta v = v$ wheel — v train). In Fig. 8 this mode of operation can be seen at 379–381 sec.
2. The second mode with constant amplitude vibrations at 61 Hz and average slip speed approximate to half of amplitude of the vibrations. In Fig. 8 this mode of operation occurs at 381–384.5 sec.
3. The third mode with vibrations at 61 Hz with rising amplitude (until slip controller reduce tractive effort). In Fig. 8 this mode of operation can be found at 384.5 sec to the end.

At time 384.5 sec is a small period of reduced vibrations, which is believed to be a small period of operation in mode 1.

The vibrations measured at frequency 61 Hz are massive in their amplitude in comparison to vibrations at 18 Hz. The largest identified amplitudes of vibrations were up to $75 - 38 = 37$ km/h at GPS speed 47 km/h. In compliance with eigenvectors of the model, the vibrations during slips similar in extent are smaller on axles 2, 3, and 5 and larger on axles 1, 4, and 6 (see Fig. 1).

The wheel speeds were carefully compared with GPS speed on straight track in sections with considerable tractive force and braking force. A determinate slip was expected to be measured, depending on actual adhesion conditions [4], but instead only negligible amount of slip was detected (less than ± 0.2 km/h). This contradicts previous concept of adhesion in wheel-rail contact.

6. SIMULATION

Simulation in MatLab with the three masses model and classic adhesion curve (depicted in Fig. 9 as **1**) was done, but the simulation results did not match the measurements. This could be because this widely used adhesion curve incorporate within itself many other aspects of wheel-rail contact, like train speed, modulation of normal force by bumps on the track [4] etc., but it is not relevant for immediate values.

Tribology uses different adhesion curve. This adhesion curve is depicted in Fig. 9 as **2**. The adhesion curve does not start at zero. This phenomenon is known as stick-slip. Because of infinite slope of the curve at zero, mathematical simulation is almost impossible; therefore a simulation was done with an adhesion curve depicted in Fig. 9 as **3**. When the immediate maximum adhesion was modulated by a random number generator there was a partial match between simulation results and

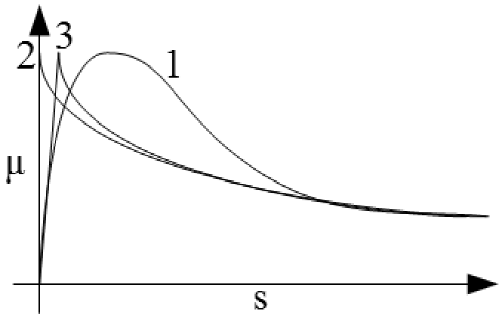

Figure 9: Adhesion characteristic.

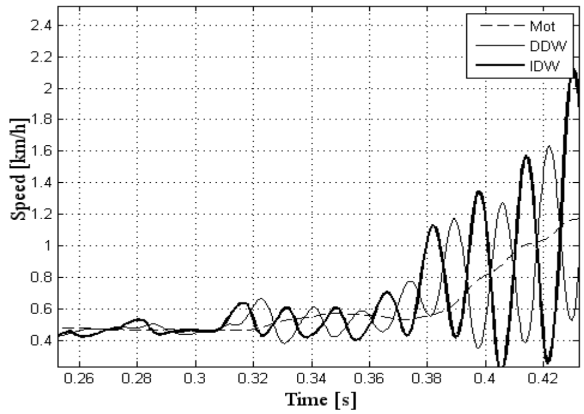

Figure 10: Simulation results.

the measurement. The simulation results depicted in Fig. 10 show sudden excitation of vibrations when one of the wheels exceed the adhesion maximum, similar to change of the operation mode from 1 to 3 (see Chapter 5). The reason why operation mode 2 (vibrations with constant amplitude) exists (is semi-stable) is unknown.

7. CONCLUSIONS

Measurements on a real locomotive show phenomenon of vibrations between the wheels instead of expected vibrations between the machine and wheels predicted by numerous physical and mathematical models. One of possible explanation could be stick-slip phenomenon known from tribology.

8. FURTHER WORK

Authors would like to make a concurrent measurement of speed on both wheels, the indirect-driven and the direct-driven, at the same time on a single axle with higher resolution. The place of the measurement will be directly on the circumference of the wheels. This will allow better understanding phase shift and amplitude between vibrations on each wheel and it will also show if there is any distortion in the speed sensor itself.

ACKNOWLEDGMENT

This work was supported by the Grant Agency of the Czech Technical University in Prague, grant No. SGS 15/079/OHK3/1T/13 Design and experimental verification of locomotive slip detection method. Many thanks go to the companies Joxima, s.r.o. and SD — Kolejová doprava, a.s. whose responsive attitude allowed realization of the measurement.

REFERENCES

1. Engel, B., H. P. Beck, and J. Alders, "Verschleißreduzierte radschlupfregelung mit hoher Kraftslußausnutzung," *Elektrische Bahnen*, Vol. 6, 201–209, 1998.
2. Engel, B., "Verschleißmindernde Kraftschlussregelung mit zustandsregler für elektrische Traktionsantriebe," Dissertation Thesis, TU, Clausthal, 1996.
3. Buscher, M., "Radschlupfregelung zur maximalen Kraftschlußausnutzung bei elektrischen Traktionsantrieben," Dissertation Thesis, Darmstadt, 1995.
4. Danzer, J., "Elektrická trakce," *Adheze*, Vol. 7, University of West Bohemia, 2010.
5. Lang, W. and G. Roth, "Optimale Kraftschlußausnutzung bei Hochleistungs-Schienenfahrzeugen," *ETR*, Vol. 42, No. 1/2, 61–66, 1993.